Am J Physiol Endocrinol Metab 306: E592–E605, 2014.
First published January 14, 2014; doi:10.1152/ajpendo.00277.2013.

Effects of insulin resistance on skeletal muscle growth and exercise capacity in type 2 diabetic mouse models

Joseph E. Ostler,[1] Santosh K. Maurya,[1] Justin Dials,[2] Steve R. Roof,[1] Steven T. Devor,[1,2] Mark T. Ziolo,[1] and Muthu Periasamy[1]

[1]*Department of Physiology and Cell Biology, The Ohio State University College of Medicine, Columbus, Ohio; and*
[2]*Department of Health Sciences, The Ohio State University College of Education and Human Ecology, Columbus, Ohio*

Submitted 20 May 2013; accepted in final form 8 January 2014

Ostler JE, Maurya SK, Dials J, Roof SR, Devor ST, Ziolo MT, Periasamy M. Effects of insulin resistance on skeletal muscle growth and exercise capacity in type 2 diabetic mouse models. *Am J Physiol Endocrinol Metab* 306: E592–E605, 2014. First published January 14, 2014; doi:10.1152/ajpendo.00277.2013.—Type 2 diabetes mellitus is associated with an accelerated muscle loss during aging, decreased muscle function, and increased disability. To better understand the mechanisms causing this muscle deterioration in type 2 diabetes, we assessed muscle weight, exercise capacity, and biochemistry in *db*/*db* and TallyHo mice at prediabetic and overtly diabetic ages. Maximum running speeds and muscle weights were already reduced in prediabetic *db*/*db* mice when compared with lean controls and more severely reduced in the overtly diabetic *db*/*db* mice. In contrast to *db*/*db* mice, TallyHo muscle size dramatically increased and maximum running speed was maintained during the progression from prediabetes to overt diabetes. Analysis of mechanisms that may contribute to decreased muscle weight in *db*/*db* mice demonstrated that insulin-dependent phosphorylation of enzymes that promote protein synthesis was severely blunted in *db*/*db* muscle. In addition, prediabetic (6-wk-old) and diabetic (12-wk-old) *db*/*db* muscle exhibited an increase in a marker of proteasomal protein degradation, the level of polyubiquitinated proteins. Chronic treadmill training of *db*/*db* mice improved glucose tolerance and exercise capacity, reduced markers of protein degradation, but only mildly increased muscle weight. The differences in muscle phenotype between these models of type 2 diabetes suggest that insulin resistance and chronic hyperglycemia alone are insufficient to rapidly decrease muscle size and function and that the effects of diabetes on muscle growth and function are animal model-dependent.

sarcopenia; ubiquitin

AS HUMANS AGE, IT IS COMMON for skeletal muscle mass and function to deteriorate (14, 22, 36). When muscle loss progresses to a pathological extreme, it is termed "sarcopenia" and contributes to physical disability (22) and prolonged hospitalizations (49). Type 2 diabetes mellitus (T2DM) is associated with an accelerated loss of muscle mass and function in the elderly (36, 37), leading to increased prevalence of clinical sarcopenia among those with T2DM. This decrease in muscle function may contribute to the 400% increased risk for major falls (31), hip fractures (31, 56), increased prevalence and severity of physical disability (11a, 15, 37, 44), and prolonged hospitalizations associated with diabetes (28).

The effects of diabetes on human skeletal muscle have been best studied in older adults in which annual loss of muscle mass is ~26% greater and annual loss of muscle strength is ~33% greater in diabetic individuals compared with those without diabetes (14, 27, 36, 37, 61). Current treatments of muscle atrophy in diabetes are limited to standard diabetic medications, improved diet, exercise, and hormonal replacement (32). Treatment of diabetes is partially effective in mitigating diabetic muscle loss; a longitudinal study in patients (60–70 yr old) using dual-energy X-ray absorptiometry found that nondiabetic individuals lost 193 g of muscle/yr, diagnosed diabetic (presumably treated) individuals lost 293 g of muscle/yr, and undiagnosed diabetic (untreated) individuals lost 435 g of muscle/yr (36). Radioisotope-based studies in humans indicate that accelerated muscle loss in patients with diabetes is caused by net protein loss associated with increased rates of muscle protein degradation (5, 16) but normal rates of meal-induced muscle protein synthesis (30). Beyond increased protein loss in diabetic humans, our understanding of diabetic muscle loss relies largely on rodent models of diabetes mellitus.

Streptozotocin-induced type 1 diabetic (T1DM) mice are the best understood model of diabetic muscle atrophy in which pharmacologically induced insulin deficiency leads to increased muscle proteasomal protein degradation and rapid muscle atrophy (39). Insulin-dependent signaling pathways are clearly important in this model, since insulin restoration (40) or phosphatase and tensin homolog ablation (18) are sufficient to rescue and prevent muscle atrophy. Blockade of glucocorticoid signaling is also sufficient to prevent muscle atrophy in streptozotocin mice, suggesting a role of glucocorticoids in diabetic muscle atrophy (19). Although convincing, these studies in T1DM mice are limited because T1DM (primary insulin deficiency) only accounts for 5–10% of cases of diabetes, with T2DM (primary insulin resistance) accounting for the remaining 90–95% of cases of diabetes mellitus (8).

Muscle atrophy in type 2 diabetic rodent models is less consistent; several models exhibit no change or mild decreases in muscle size [i.e., high-fat diet (50, 60, 65), muscle insulin receptor knockout (12), insulin receptor substrate (IRS)-1 knockout (29), and IRS-2 knockout (29)], whereas several models demonstrate severely reduced muscle size [leptin deficient (*ob*/*ob*) (24, 53, 63), leptin receptor deficient (*db*/*db*) (62), muscle specific IRS-1/IRS-2 knockout (29)]. The most detailed rodent studies of type 2 diabetic muscle atrophy have focused on the *ob*/*ob* and *db*/*db* mouse models.

The *ob*/*ob* mouse (leptin mutant) is hyperphagic, severely obese (20), hyperinsulinemic, and hyperglycemic (58). The adult *ob*/*ob* mouse has severely reduced weight of fast and mixed skeletal muscles compared with age-matched wild-type (WT) controls but has normal slow (soleus) muscle weight (24, 53, 63). The preferential effects on fast muscle in *ob*/*ob* mice

Address for reprint requests and other correspondence: M. Periasamy, 300 Hamilton Hall, 1645 Neil Ave., Columbus, OH 43210 (e-mail: Muthu.periasamy@osumc.edu).

are emphasized by the marked reduction in cross-sectional area (CSA) and proportion of fast glycolytic fibers, with no change in CSA or proportion of slow oxidative fibers (3). Functionally, *ob*/*ob* muscle maintains WT levels of whole muscle and single fiber force production when normalized to CSA but demonstrates decreased rates of relaxation and premature fatigue during induced tetanus compared with WT (7). Reduced satellite cell proliferation during early postnatal development (41) and in response to chemical injury (33) has been reported in *ob*/*ob* mice. Although leptin administration in adult *ob*/*ob* mice normalizes glycemia (46) and partially restores muscle mass (45), pair feeding adult *ob*/*ob* mice does not improve muscle mass (45), despite a moderate lowering of blood glucose levels (46).

The *db*/*db* mouse (leptin receptor mutant) metabolic phenotype is similar to the *ob*/*ob* mouse, presenting with hyperphagia, juvenile-onset obesity, and diabetes (9). Depending on background genetic strain, *db*/*db* mice exhibit pancreatic islet hyperplasia [C57BL/6J (13)] or islet atrophy [C57BL/KsJ (23)]; pancreatic islet atrophy results in a more severe diabetic phenotype, late-onset weight loss, and a shortened lifespan compared with *ob*/*ob* mice. *db*/*db* mice also exhibit reduced skeletal muscle size, increased muscle protein degradation, elevated proteasome function, and reduced muscle fiber CSA (62). Glucose intolerance and reduced muscle size in *db*/*db* mouse is partially normalized by chronic rosiglitazone treatment, suggesting a role of metabolism in the reduced muscle size (62).

Taken together, these previous findings suggest that T2DM is associated with fast glycolytic skeletal muscle loss that is partially reversed by interventions that improve metabolism [such as rosiglitazone in *db*/*db* mice (62), leptin in *ob*/*ob* mice (45), or antidiabetic treatment in humans (36)]. The ability of insulin to completely rescue muscle atrophy in T1DM mice (40) suggests that decreased insulin signaling could directly cause muscle loss in T2DM. Canonical insulin signaling promotes protein synthesis [via protein kinase B (Akt)/mammalian target of rapamycin (mTOR)] and inhibits protein degradation [via Akt/forkhead box O (FOXO) signaling] (57); it is logical that insulin resistance could reduce protein synthesis and increase protein degradation. However, it is unclear if decreased insulin signaling in T2DM directly causes muscle loss or if other diabetes-associated factors drive muscle atrophy. Indeed, the onset, progression, biochemical phenotype, and causative signaling pathways for muscle loss in T2DM remain unclear.

Therefore, to better understand the progression and causal mechanisms of muscle atrophy in T2DM, we compared muscle growth/loss in both the well-characterized *db*/*db* and the less-characterized TallyHo mouse models of T2DM. The TallyHo model was studied because it is a polygenic model of overt T2DM with intact leptin signaling. Moreover, TallyHo mice develop diabetes at a mature age, allowing us to investigate the impact of insulin resistance and hyperglycemia on mature muscle, which is more clinically relevant compared with the juvenile onset of diabetes in *db*/*db* mice. We also studied how a common treatment for diabetes (chronic exercise) affects muscle size, glucose tolerance, and markers of muscle protein synthesis and degradation in *db*/*db* mice. We hypothesized that delineating the onset of muscle atrophy in these models of T2DM as well as the effects of exercise would help clarify which components of the diabetic phenotype are sufficient to cause muscle loss in T2DM.

RESEARCH DESIGN AND METHODS

Animals

Male *db*/*db* (BKS.Cg-Dock7m$^{+/+}$ Leprdb/J), age-matched WT controls (C57BLKS/J), and TallyHo (TallyHo/JngJ) mice were purchased from Jackson Laboratories (Bar Harbor, ME). Because TallyHo mice were originally created at Jackson Labs by selective crossbreeding of multiple strains of mice, no accurate control strain of mice exists to compare with TallyHo mice (26). To overcome this challenge, 8-wk-old TallyHo mice were studied to establish a prediabetic baseline to compare with the 22- to 24-wk-old overtly diabetic TallyHo mice. Obesity was induced in select WT C57BLKS/J mice by providing a high-fat diet (HFD, 4.73 kcal/g, 45% kcal from fat; D12451; Research Diet, New Brunswick, NJ) from the age of 8 wk until their death at 20 wk old, whereas all other mice were fed standard chow diet (3.0 kcal/g, 4.25% kcal from fat), as described previously (4). Male mice only were used because of the relatively homogeneous metabolic phenotype of males compared with females in the *db*/*db* and TallyHo mouse models. The mice were maintained on a 12:12-h light-dark cycle with ad libitum access to food and water, except when fasted (described below). Mice were killed by CO_2 exposure. All animal experiments were approved by The Ohio State University Institutional Animal Care and Use Committee.

Glucose Tolerance Test

After an overnight fast (*db*/*db* mice) or 6-h fast (TallyHo mice), fasting blood glucose levels were measured using tail blood in a TRUEtrack blood glucose monitoring kit (Walgreens, Columbus, OH). The maximum physical limit of the glucometer was 33.3 mM; glucose levels >33.3 mM (reading as "HI") were treated as 33.3 mM for facility of quantitative data comparison. An injection of glucose (2 g/kg ip; Sigma-Aldrich), dissolved in Dulbecco's phosphate-buffered saline (DPBS; Invitrogen, Carlsbad, CA), was given to each mouse, and blood glucose measurements were obtained at 30, 60, 90, 120, and 240 min postinjection. Glucose tolerance tests were compared by calculating the integrated area under the curve (AUC) of the blood glucose level for the 240 min of the test.

Measurement of Body Size and Muscle Weight

Body weight was determined in a fed state. To determine muscle weight, after death by CO_2 inhalation, muscles were carefully dissected, and tendons were removed to the beginning edge of muscle tissue. Muscles were briefly immersed in DPBS, dabbed on tissue paper to remove excess fluid, weighed on a digital analytical balance, and then frozen in liquid nitrogen.

Maximal Oxygen Consumption Treadmill Test

Maximum cardiopulmonary function and running speeds were assessed using a Metabolic Modular Treadmill (Columbus Instruments, Columbus, OH) as described previously (55), with several modifications to adapt to the poor exercise capacity of the *db*/*db* mice, as follows.

Acclimation. Mice were acclimated to the treadmill 1–3 days before testing by being placed on an unmoving treadmill for 3 min, after which the shock grid was activated (3 Hz and 1.5 mA) and the treadmill was engaged to a walking speed of 6 m/min for 5 min.

Maximal oxygen consumption test. Mice were placed on the treadmill (0° incline entire experiment), and the shock grid was activated. The treadmill speeds were then increased until exhaustion as follows: speed, duration, 0 m/min, 5 min; 6 m/min, 5 min; 7, 8, 9, and 10 m/min, 30 s each; 11 m/min, 1 min; 12, 13, 14, and 15 m/min, 2 min each; and +1 m/min, each 1 min thereafter. Exhaustion (endpoint for treadmill cessation) was defined as the point at which mice maintained continuous contact with the shock grid for 5 s. Maximal oxygen consumption ($\dot{V}O_{2max}$) was determined by the peak oxygen consump-

tion reached during this test when the respiratory quotient was >1.0. Maximum running speed was defined as the treadmill speed at which $\dot{V}O_{2max}$ was achieved.

Voluntary Activity Measurements

Mouse activity levels were measured using measurement of horizontal infrared beam breaks over the course of 24 h using an Comprehensive Lab Animal Monitoring System at room temperature (CLAMS; Columbus Instruments).

Grip Strength Test

Forelimb grip strength was assessed using a digital Grip Strength Meter (Columbus Instruments). Mice were lifted by their tails, allowed to grasp the forelimb pull bar, and pulled smoothly away from the transducer in the horizontal plane, and maximum force exerted on the transducer was recorded. This test was repeated in 3 sets of 10 attempts, with a 15-min rest in between sets; the maximum effort recorded from all attempts by each mouse was designated as maximum grip strength.

Insulin Acute Response Test

To assess tissue-specific acute responses to insulin, basal tail blood glucose was assessed, and then recombinant human insulin (Humulin, 0.2 U/g body wt ip; Eli Lilly, Indianapolis, IN) or DPBS was administered to select mice. Ten minutes after injection, tail blood glucose was assessed, the mice were immediately killed, and tissues were removed.

Chronic Exercise

Mice were exercised from 5 to 13 wk of age using the interval training method as described previously (55), with slight modifications. Mice were treadmill exercised 80 min/day, 5 days/wk, for 8 wk. Training was performed on a 20° incline, alternating 4 min high speed and 2 min low speed (high = 80–90% of speed at which $\dot{V}O_{2max}$ was reached, slow = 50% of speed at which $\dot{V}O_{2max}$ was reached). The $\dot{V}O_{2max}$ tests for the exercised mice and their controls were performed as described above but with the following changes to speed/incline to determine appropriate training speeds for running on an incline: speed, duration, incline, 0 m/min, 5 min, 0°; 6 m/min, 5 min, 0°; 6 m/min, 2 min, 20°; and +2 m/min, each 2 min thereafter, 20°. At the end of the study, mice were killed in a fed state 3–5 days after the last bout of exercise. No exogenous insulin was administered to the mice.

Protein Quantification Using Western Blotting

Western blotting was carried out using standard techniques, as described previously (4). Protein concentrations of total homogenate were determined by the Bradford method, and equivalent amounts of protein were loaded in each lane of the polyacrylamide gel. After electrophoresis, protein were transferred to 0.45-μM nitrocellulose membranes and stained with the Ponceau stain (0.1% wt/vol Ponceau Red in 5% acetic acid) to visualize protein loading. Membranes were washed with Tris-buffered saline containing 0.5% Tween 20 (TBS-T) and blocked for nonspecific binding [room temperature (RT), 2 h, 5% (wt/vol) nonfat milk in TBS-T]. Membranes were probed with primary antibodies for either 3 h at RT or overnight at 4°C, at the following dilutions: sarco(endo)plasmic reticulum Ca^{2+}-ATPase (SERCA) 1a, 1:5,000, custom-made antibody; SERCA2a, 1:5,000, custom-made antibody; α-actin, 1:25,000; CSQ, 1:5,000; phospho-Akt, 1:2,000 ($pSer^{473}$, Clone D9E XP; Cell Signaling Technology, Danvers, MA); Akt, 1:2,000; MuRF-1, 1:1,000 (AP2041; ECM Biosciences, Versailles, KY); atrogin-1, 1:1,000 (MP3401; ECM Biosciences); p-4E-binding protein 1 (4EBP-1), 1:5,000 ($pThr^{37/46}$, Clone 236B4; Cell Signaling Technology); p70S6K, 1:5,000 ($pThr^{389}$, Clone 108D2; Cell Signaling Technology); pS6, 1:5,000 ($pSer^{235/236}$, Clone D57.2.2E XP; Cell Signaling Technology); phospho-mTOR, 1:2,000 (2971S, $pSer^{2448}$; Cell Signaling Technology); pFOXO1, 1:1,000 ($pSer^{256}$; Cell Signaling Technology); anti-pan ubiquitin, 1:1,000 (clone FK2; Cell Signaling Technology); and anti-poly-ubiquitin, Lys^{48}-specific, 1:5,000 (clone Apu2; Millipore, Temecula, CA). After being washed with 0.05% TBS-T, blots were probed with the appropriate horseradish peroxidase-linked secondary antibody for 1 h at RT and then washed again with 0.05% TBS-T, developed with enhanced chemiluminescent substrate (SuperSignal West Dura Chemiluminescent Substrate; Thermo Fisher Scientific, Rockport, IL), and exposed to film. Blots were scanned (HP Imaging), and relative protein quantitation was performed by densitometry using the middle third of each band, normalizing by the relative intensity of the loading control bands (α-actin or Ponceau stain), using Image J analysis software (National Institutes of Health) (42).

Corticosterone and Inflammatory Cytokine Arrays

Blood was collected from 16-wk-old WT C57BLKS/j mice, 16-wk-old *db*/*db* mice, and 8-mo-old TallyHo mice between 0900 and 1000 in a fed state. Five minutes prewarming of the mice in a 37°C temperature-controlled cage was used to enhance tail blood flow and facilitate rapid collection of adequate blood. Blood was collected in <2 min from the tail veins to minimize potential of handling-induced changes in glucocorticoid/inflammatory signaling. Serum was analyzed for free corticosterone using a corticosterone ELISA kit (ADI-900–097; Enzo Life Sciences, Farmingdale, NY), following the manufacturer's instructions. Relative levels of serum inflammatory proteins were determined using the Mouse Cytokine Antibody Array Panel A (R&D Systems, Minneapolis, MN), per the manufacturer's instructions.

Histology. Muscles (n = 2–5) were gently rinsed in DPBS, dabbed on tissue paper to remove excess moisture, and then stored in 10% (vol/vol) formalin. Tissue was then paraffin embedded, cut, and stained with hematoxylin/eosin or the Masson-Trichrome stain using standard techniques. Images were obtained using a light microscope at ×20 magnification (Zeiss Axioskop 40, Oberkochen, Germany). Fiber CSA was quantified using Axiovision LE software (Zeiss, Oberkochen, Germany), with at least 90 contiguous fibers quantified per sample.

Data Interpretation

Statistically significant data were identified by use of the two-sided Student's t-test, $\alpha = 0.05$. All metabolic, functional, and biochemical tests were performed on at least three to four animals per condition. Western blots were repeated in at least duplicate.

RESULTS

A major objective of this study was to identify what components of the diabetic phenotype are necessary for muscle loss in type 2 diabetes. To this end, we took advantage of the type 2 diabetic male *db*/*db* and TallyHo mouse models, which exhibit overt type 2 diabetes at ~8 and ~14 wk of age, respectively (62). We investigated the relationship of diabetic state to muscle mass and function by comparing mice at approximately prediabetic and overtly diabetic ages.

Progression of Metabolic Phenotype in db/db Mice

First, we confirmed the development of the diabetic phenotype in *db*/*db* mice at 6 and 12 wk of age compared with age-matched WT controls. Total body weight in *db*/*db* mice was moderately elevated in 6-wk-old mice and severely increased in 12-wk-old mice compared with controls (Fig. 1*A*). Fasting blood sugar was mildly increased in 6-wk-old (8.3 ± 0.6 mM WT vs. 13.8 ± 1.8 mM *db*/*db*, $P < 0.05$) and severely increased in 12-wk-old *db*/*db*

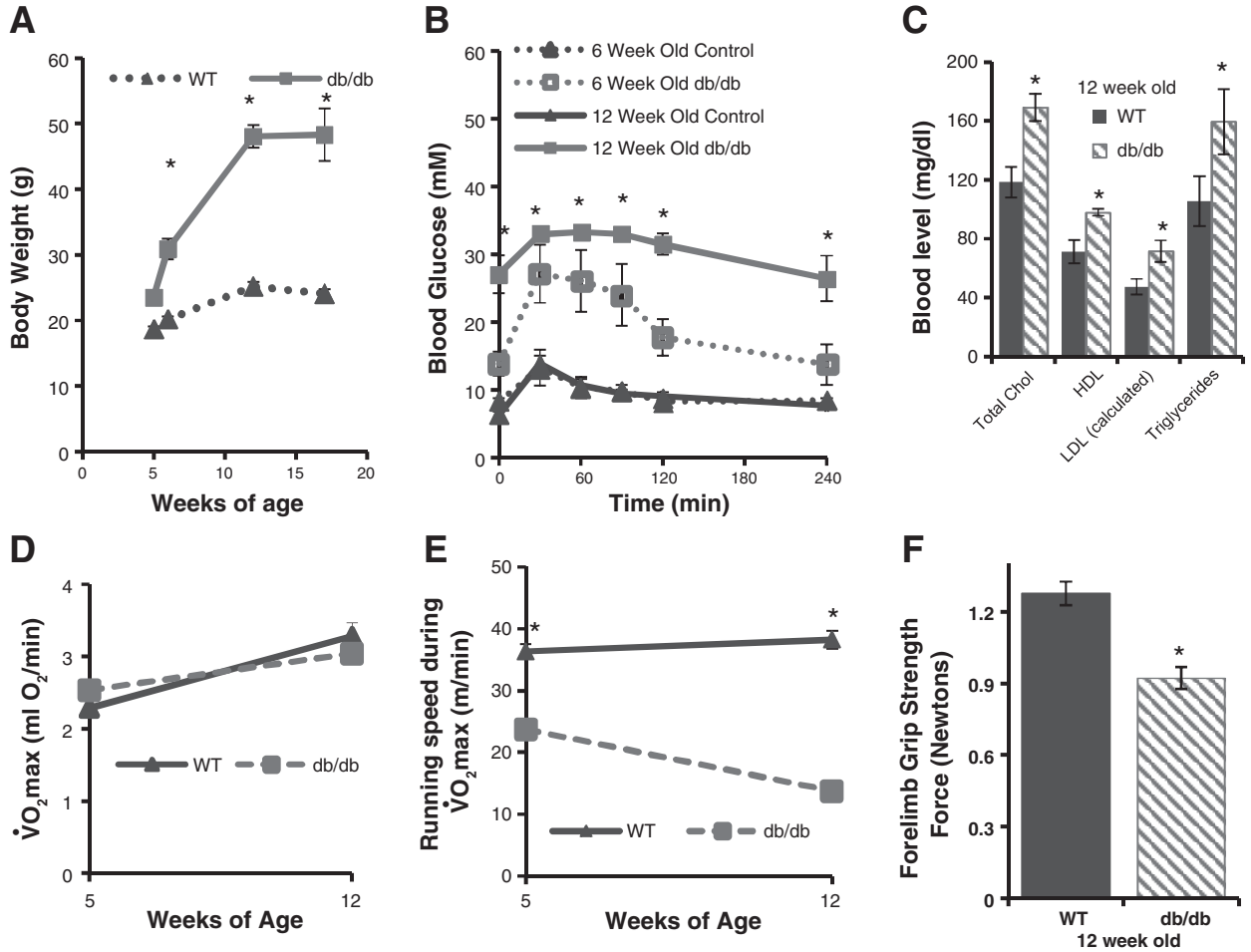

Fig. 1. Development of obesity, glucose intolerance, and decreased exercise capacity in *db*/*db* male mice. *A*: *db*/*db* mice gain body weight more quickly than wild-type (WT) mice beginning at 5 wk of age. *B*: glucose tolerance progressively deteriorates in *db*/*db* mice from 6 to 12 wk of age. *C*: 12-wk-old *db*/*db* mice present with elevated fasting serum cholesterol and triglycerides. HDL, high-density lipoprotein; LDL, low-density lipoprotein. *D*: maximum cardiopulmonary capacity ($\dot{V}O_{2max}$) is not significantly altered in 5- or 12-wk-old *db*/*db* diabetic mice compared with age-matched WT. *E*: the maximum running speed achieved during the $\dot{V}O_{2max}$ test is significantly lower in *db*/*db* mice compared with WT, both at 5 and 12 wk of age. *F*: forelimb grip strength is significantly reduced in 12-wk-old *db*/*db* mice. Error bars = SE. $^*P < 0.05$ compared with WT.

mice compared with WT controls (6.3 ± 0.6 mM WT vs. 27.1 ± 2.8 mM *db*/*db*, $P < 0.05$). Glucose tolerance was moderately impaired in 6-wk-old *db*/*db* mice (AUC 38.1 ± 2.6 mM·h WT vs. 78.0 ± 9.3 mM·h *db*/*db*, $P < 0.05$) but was more severely impaired in 12-wk-old *db*/*db* (AUC 37.7 ± 1.8 mM·h WT vs. 122.3 ± 5.7 mM·h *db*/*db*, $P < 0.05$) mice (Fig. 1*B*). Fasted 12-wk-old *db*/*db* mice exhibited elevated blood levels of total cholesterol, high-density lipoprotein, low-density lipoprotein, and triglycerides (Fig. 1*C*). These findings are consistent with what has been reported previously (9). Based on these findings, we chose to study changes in *db*/*db* skeletal and cardiac muscle at prediabetic (5–6 wk old) and "overtly diabetic" (12–13 wk old) states.

Decline of Exercise Capacity of db/db Mice

The functional decline of cardiac and skeletal muscle was determined by assessing $\dot{V}O_{2max}$ during forced treadmill running. No significant impairment in maximum cardiac function ($\dot{V}O_{2max}$) was observed in 6-wk-old prediabetic or 12-wk-old overtly diabetic *db*/*db* mice compared with age-matched WT controls (6 wk old 2.28 ± 0.01 ml O_2/min WT vs. 2.54 ± 0.08 ml O_2/min *db*/*db*; 12 wk old 3.28 ± 0.18 ml O_2/min WT vs. 3.04 ± 0.10 ml O_2/min *db*/*db*, $P > 0.05$) (Fig. 1*D*). The maximum running speed was reduced by 34.6% at 6 wk old and 64.1% at 12 wk old (6 wk old 36 ± 1 m/min WT vs. 24 ± 1 m/min *db*/*db*; 12 wk old 38 ± 1 m/min WT vs. 13.8 ± 0.9 m/min *db*/*db*, $P < 0.05$) (Fig. 1*E*). Depressed skeletal muscle functional capacity was confirmed by measuring in vivo forelimb grip strength, which was reduced in 12-wk-old *db*/*db* mice by 28% compared with age-matched WT controls (1.27 ± 0.05 Newton WT vs. 0.92 ± 0.05 Newton *db*/*db*, $P < 0.05$) (Fig. 1*E*).

Progression of Metabolic Phenotype TallyHo Mice

The TallyHo male mouse is a leptin-intact, mature-onset, and polygenic (52) model of T2DM that develops reduced insulin-dependent muscle glucose uptake by 6 wk of age, whole body insulin resistance at ~8 wk of age, and overt hyperglycemia at ~16 wk of age (26). Based on published literature (25, 26, 52), we selected 8- to 9-wk-old and 22- to 24-wk-old TallyHo male mice to compare the muscle phenotype at prediabetic and overtly diabetic stages, respectively. First, the TallyHo metabolic phenotype was confirmed to validate the comparison. TallyHo mice gained body weight

during this time period (31.6 ± 0.5 g 8 wk old vs. 36.4 ± 0.7 g 24 wk old). In addition, fasting hyperglycemia was present in prediabetic 8-wk-old mice (15.9 ± 1.5 mM fasting blood glucose) and became significantly higher in the overtly diabetic 23-wk-old mice (21.0 ± 2.5 mM, $P < 0.05$). Glucose tolerance of TallyHo mice was already impaired in the prediabetic TallyHo and more severely impaired in the overtly diabetic TallyHo mice. This gradual mature onset of diabetes agrees with previous findings (26).

Exercise Capacity of TallyHo Mice

The exercise capacity of TallyHo mice did not decrease with the onset of overt diabetes (Fig. 2). Specifically, maximum cardiac capacity increased with age between the prediabetic 7-wk-old and overtly diabetic 22-wk-old TallyHo mice (3.07 ± 0.02 ml O_2/min 7 wk old TallyHo vs. 3.68 ± 0.08 ml O_2/min 22 wk old TallyHo) (Fig. 2*C*). In addition, maximum running speed achieved during the tests was not significantly different between the age groups (31 ± 1 m/min 7 wk old TallyHo vs. 29.5 ± 0.6 m/min 22 wk old TallyHo, $P > 0.05$) (Fig. 2*D*).

Muscle Weight is Reduced Significantly in db/db Mice but not in the TallyHo Mouse Model

To understand the poor running speed and grip strength of *db*/*db* mice, muscle weight and histology were assessed. Hindlimb muscle size was visibly reduced in 6- and 12-wk-old *db*/*db* mice compared with WT controls (Fig. 3*A*). No increase in centrally located nuclei (which would suggest muscle injury and regeneration) was evident in *db*/*db* tibialis anterior muscle by histology (Fig. 3, *A* and *B*). Wet muscle mass was decreased in predominantly fast-type skeletal muscle (gastrocnemius, tibialis anterior, and extensor digitorum longus) from prediabetic 6-wk-old mice and more so in overtly diabetic 12-wk-old mice. Notably, although the disparity between *db*/*db* and WT mice muscle weight increased with age, *db*/*db* muscle weight increased throughout this period, but at a much lower rate than WT controls. This suggests decreased muscle growth and not muscle loss as the cause of decreased *db*/*db* muscle weight. No significant change was evident in *db*/*db* tibia length, cardiac weight, or soleus weight (predominantly slow oxidative muscle) compared with WT controls (Table 1). Average muscle fiber CSA was decreased in fast-type muscle (tibialis anterior) but not in slow oxidative muscle (soleus) (Fig. 3, *D* and *E*).

On the other hand, TallyHo skeletal and cardiac muscle weight and tibia length increased from 9 wk of age to 24 wk of age mice despite glucose intolerance and hyperglycemia (Table 1). Comparison of Tallyho muscle weight with "healthy" muscle weight is limited to using prediabetic TallyHo because of the lack of available nondiabetic controls for TallyHo mice [because of extensive crossbreeding between different strains to develop this polygenic model (26)]. Moreover, average muscle weight and fiber CSA of both predominantly slow muscle (soleus) and fast muscle (tibialis anterior) were increased compared with C57BLK/s WT controls (Fig. 3, *D* and *E*). No evidence of increased centrally located nuclei was observed in TallyHo muscle by histology (Fig. 3*B*). Masson trichrome staining did not indicate increased fibrosis in diabetic *db*/*db* or Tallyho tibialis anterior muscle (Fig. 3*C*).

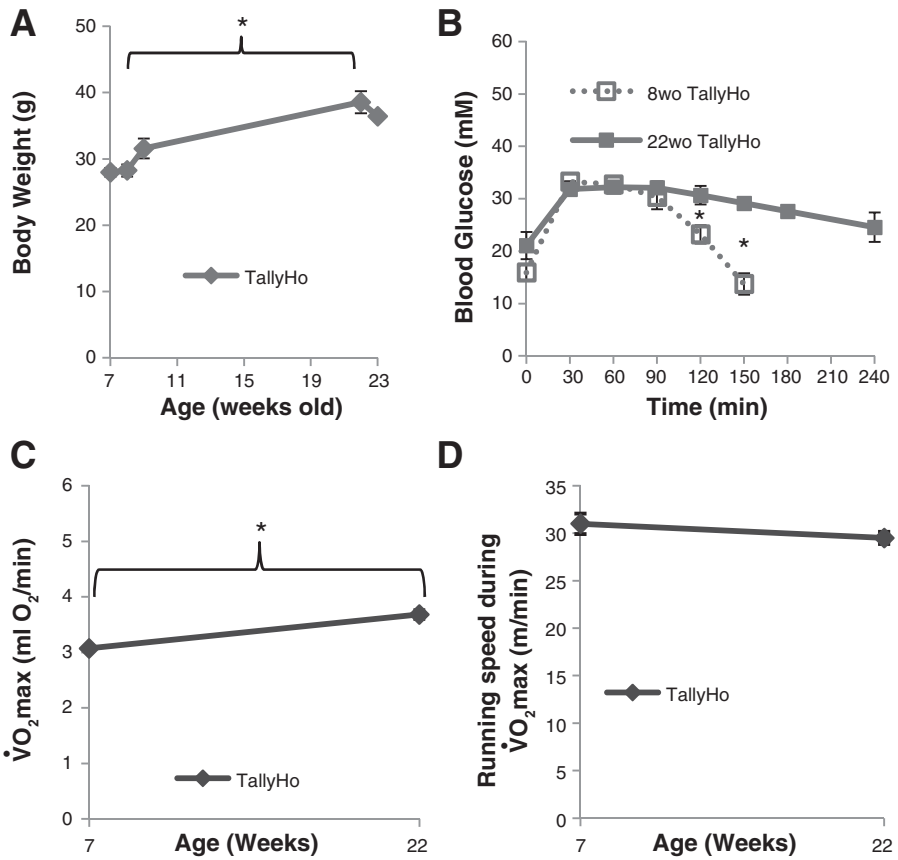

Fig. 2. Development of obesity and glucose intolerance but maintenance of exercise capacity in TallyHo mice. *A*: TallyHo mice increase in body weight from 8 to 24 wk of age. *B*: glucose tolerance is impaired in 8-wk-old TallyHo and further deteriorates in the 22-wk-old TallyHo mice. *C*: maximum cardiopulmonary capacity ($\dot{V}O_{2max}$) increases with age in TallyHo mice between 7 and 22 wk of age. *D*: the maximum running speed recorded during the $\dot{V}O_{2max}$ test by 7-wk-old TallyHo mice is still achieved by the overtly diabetic 22 wk. Error bars = SE. *$P < 0.05$ compared with young TallyHo.

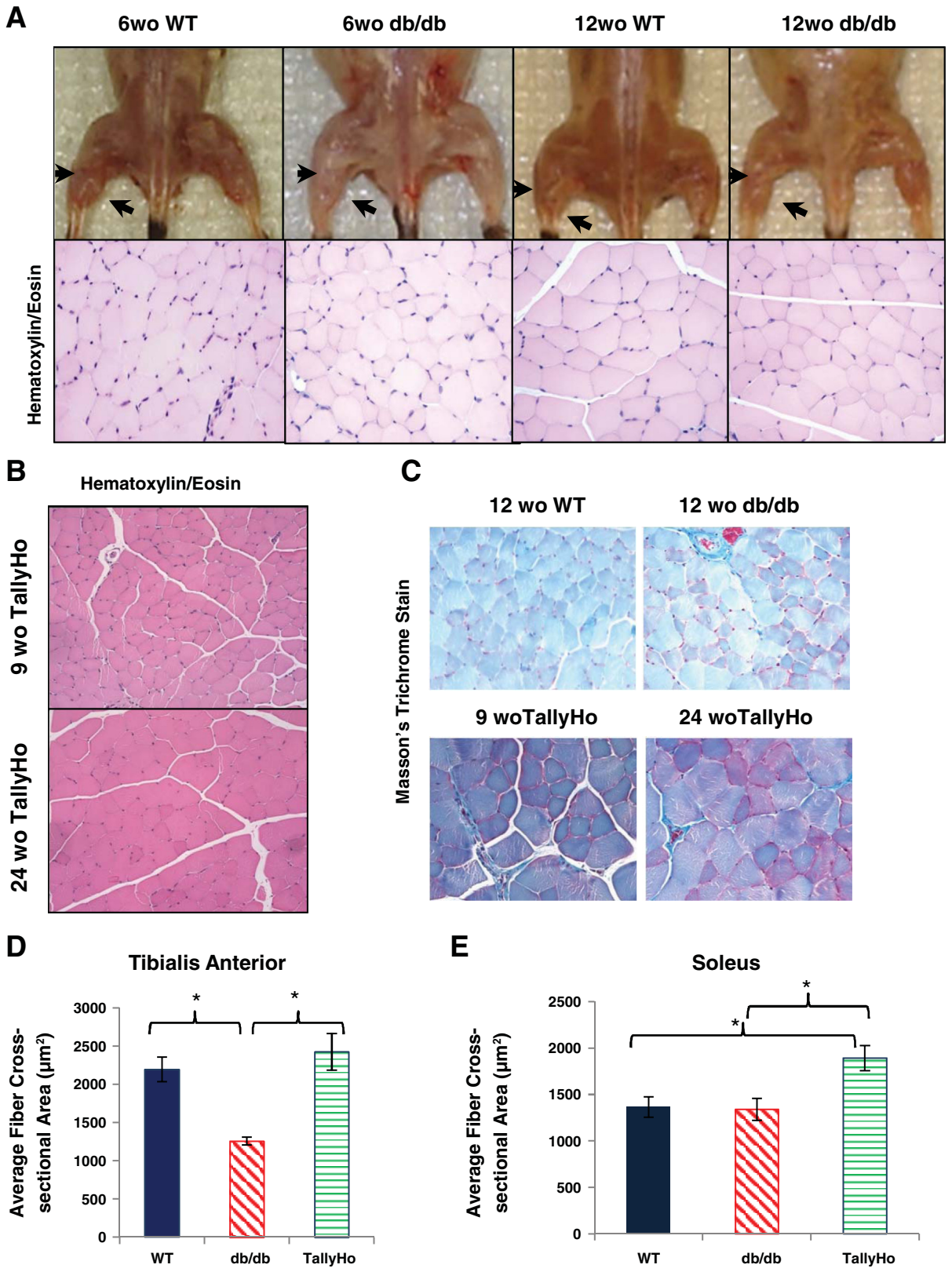

Fig. 3. Visually reduced muscle size of *db*/*db* mice and histology of *db*/*db* and TallyHo mice muscle. *A*: apparent muscle size is severely decreased in *db*/*db* mice relative to age-matched controls at 6 and 12 wk of age (wo). *B*: hematoxylin and eosin staining does not demonstrate an increase in centrally located nuclei in *db*/*db* or TallyHo tibialis anterior muscle. *C*: Masson's trichrome staining does not demonstrate a visibly apparent increase in collagen staining (blue) in tibialis anterior muscle sections from overtly diabetic *db*/*db* or TallyHo mice. *D* and *E*: in *db*/*db* mice, muscle fiber cross-sectional areas are reduced in fast glycolytic tibialis anterior muscle (*D*) but not slow oxidative soleus muscle (*E*) compared with age-matched WT controls. TallyHo fiber cross-sectional area is increased in both fast (*D*) and slow (*E*) muscle types compared with WT controls. $*P < 0.05$ compared with WT.

Table 1. *Body weight, muscle weights, and tibia size in prediabetic and diabetic db/db and TallyHo mice*

	n	Body Wt, g	Ventricles, mg	Gastrocnemius, mg	Tibialis Anterior, mg	Extensor Digitorum Longus, mg	Soleus, mg	Tibia Length, mm
9-wk-old TallyHo	4	31.7 ± 0.9	108.8 ± 0.6	114.1 ± 2.8	44.4 ± 1	8.1 ± 0.7	6.2 ± 0.2	17.4 ± 0.3
24-wk-old TallyHo	6	37.7 ± 1.6‡	172.3 ± 9.1‡	150.3 ± 4.5‡	53.6 ± 0.9‡	12.2 ± 0.3‡	9.5 ± 0.4‡	19.2 ± 0.2‡
6 wk C57BLKS control	4	20.2 ± 0.4	97.5 ± 4.2	91.1 ± 6.1	32.7 ± 0.9	6 ± 0.3	4.7 ± 0.3	7 ± 0.7
6-wk-old *db/db* Diabetic	4	30.9 ± 1.6*	86.7 ± 4.3	60.5 ± 8.4*	27.8 ± 0.9*	5.1 ± 0.3	5.1 ± 0.3	6.3 ± 1
12-wk-old C57BLKS control	4	25.4 ± 0.8	117.2 ± 4	128.4 ± 3.6	42.9 ± 2.3	10.4 ± 0.7	6.4 ± 0.5	18.7 ± 0.3
12-wk-old *db/db* Diabetic	4	48.9 ± 1.2*	117.6 ± 4.9	71.9 ± 2.5*	26.5 ± 1.9*	6.8 ± 0.5*	6.3 ± 0.6	18.4 ± 0.2
13-wk-old C57BLKS control	4	21.5 ± 0.40	NM	132 ± 3.7	53.6 ± 1.9	NM	NM	NM
13-wk-old *db/db* Sedentary	8	47.7 ± 2.5*	NM	63.3 ± 1.4*	30.3 ± 0.9*	NM	NM	NM
13-wk-old *db/db* Exercised	8	46.8 ± 1.4*	NM	77 ± 3*†	28.6 ± 0*	NM	NM	NM

The values are means ± SE; *n*, no. of mice. Body weight, tibia length, and all muscle weights are increased in diabetic 24-wk-old TallyHo compared to prediabetic 9-wk-old TallyHo mice. Fast muscle weight is reduced in both 6- and 12-wk-old *db/db* mice compared with age-matched wild-type (WT) controls. Mice that have been chronically exercised for 8 wk do not have significantly different body weight or tibialis anterior weight but do have a mild yet significant increase in weight of gastrocnemius muscle compared with sedentary *db/db* mice. NM, not measured. *$P < 0.05$ compared with age-matched WT. †$P < 0.05$ compared with age-matched sedentary *db/db*. ‡$P < 0.05$ compared with 9-wk-old TallyHo.

Decreased Insulin-Dependent Phosphorylation of Regulators of Protein Synthesis in db/db Muscle

To better understand the mechanisms causing decreased muscle size in the *db/db* diabetic model, insulin-dependent regulation of protein synthetic pathways was assessed. A single intraperitoneal injection of insulin in overnight-fasted mice acutely increased phosphorylation of proteins key to activating protein synthesis (Akt, mTOR, 4EBP-1, p70S6K, and S6 proteins). Basal levels of phosphorylation of these proteins was generally slightly greater in WT mice, with the exception of 4EBP-1, which demonstrated greater basal phosphorylation in *db/db* muscle compared with muscle from WT mice (Fig. 4). Upon stimulation with insulin, WT mice displayed a robust increase in phosphorylation of these protein synthetic pathways in tibialis anterior, diaphragm, and ventricular muscle, with the exception of mTOR in the diaphragm. In *db/db* mice, insulin-dependent phosphorylation of these regulators of protein synthesis, although evident, was markedly reduced in slow/mixed (diaphragm), fast (tibialis anterior), and cardiac muscle. These data expand upon previous literature (47) and demonstrate that insulin-dependent activation of pathways regulating protein synthesis is blunted in muscles of adult *db/db* mice. Although the single intraperitoneal insulin bolus was sufficient to activate insulin-dependent signaling pathways 10 min after insulin injection, no significant reduction of blood glucose concentrations in WT or *db/db* mice occurred during this time; this may indicate that, although some intracellular pathways are activated at this time point, glucose transport has not been increased sufficiently to alter blood glucose concentrations.

Increased Ubiquitinated Proteins and Atrophy-Associated E3 Ubiquitin Ligases in Diabetic Muscle

We next studied the role of proteasomal protein degradation in decreased muscle size and function in *db/db* mice. Previous literature has shown protein degradation rates and 26S proteasome function to be elevated in muscle from 9-wk-old *db/db* mice (62). We examined how increased proteasomal protein degradation, as observed by accumulation of polyubiquitinated proteins (64), progresses with decreased muscle size and function in prediabetic and overtly diabetic mice. Western blotting of whole muscle homogenate with an anti-k48-polyubiquitin specific antibody revealed a clear increase in the quantity of polyubiquitin-conjugated proteins over the observed range of 25–250 kDa in *db/db* muscle. Accumulation of polyubiquitinated proteins was already significantly increased in fast, slow, and cardiac muscles from prediabetic *db/db* mice (gastrocne-

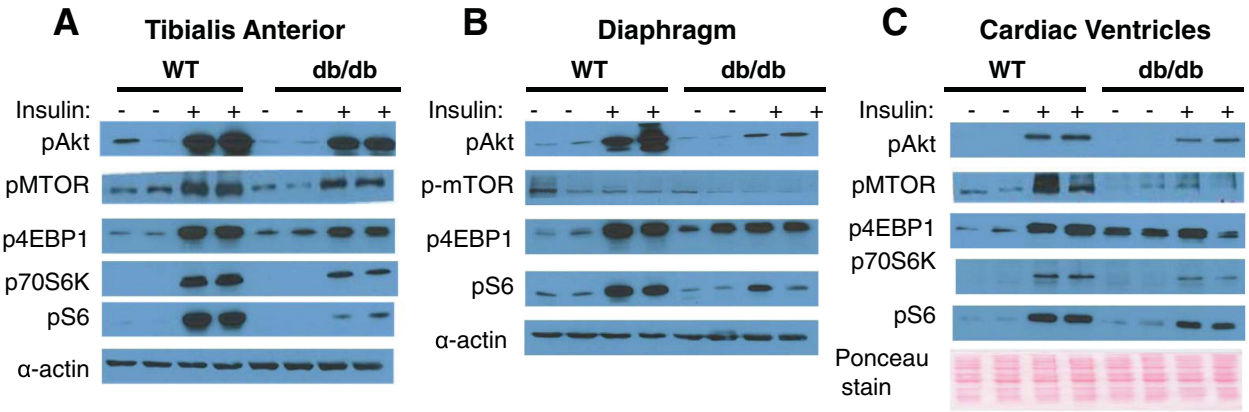

Fig. 4. Reduced insulin-dependent phosphorylation of regulators of protein synthesis in diabetic muscle. *A–C*: fast (tibialis anterior) (*A*), slow (diaphragm) (*B*), and cardiac (*C*) muscle from 12-wk-old overtly diabetic *db/db* mice exhibit a reduced response to a single in vivo bolus injection of insulin (0.2 U/g body wt, recombinant human insulin ip, 10 min) compared with lean WT controls, as evidenced by decreased insulin-dependent phosphorylation of key promoters of protein synthesis [protein kinase B (Akt), mammalian target of rapamycin (mTOR), 4E-binding protein 1 (4EBP1), p70S6K, and S6]. Skeletal α-actin and the Ponceau stain for cardiac tissue are loading controls.

mius, soleus, and ventricle) and further increased in these muscles from the overtly diabetic *db/db* mice (Fig. 5, *A–C*).

Decreased Insulin-Dependent FOXO1 Activation and Increased Expression of MuRF-1, Atrogin-1 in db/db Muscle

MuRF-1 and atrogin-1 are well-studied E3 ubiquitin ligases that catalyze a rate-limiting step of protein ubiquitination that labels the substrate protein for subsequent proteasomal protein degradation. Of the large family of E3 ligases, MuRF-1 and atrogin-1 are notable for their role in being associated with and partially necessary for many types of muscle atrophy (6). Western blotting showed a statistically insignificant trend toward increased levels of E3 ubiquitin ligases Murf-1 and atrogin-1 in fast (tibialis anterior) and slow/mixed (soleus) muscle from 12-wk-old *db/db* mice compared with age-matched WT mice (Fig. 5*F*).

FOXO Family Signaling Promotes Transcription of Atrogin-1 and MuRF-1

Insulin-dependent phosphorylation of FOXO1 is associated with deactivation of transcriptional activity by translocation of FOXO1 out of the nucleus. We found that insulin-dependent phosphorylation of FOXO1 was blunted in the tibialis anterior, diaphragm, and the cardiac muscles of 12-wk-old *db/db* mice compared with WT controls (Fig. 5*D*).

Increased Accumulation of Polyubiquitinated Proteins Is Not Found in Muscle from TallyHo and HFD Models of Insulin-Resistant Diabetes

To test if the accumulation of polyubiquitinated proteins is a feature common to diabetes in general, or just specific to *db/db* mice, we tested two additional models of insulin-resistant diabetes (Fig. 5*E*). We found that the levels of polyubiquiti-

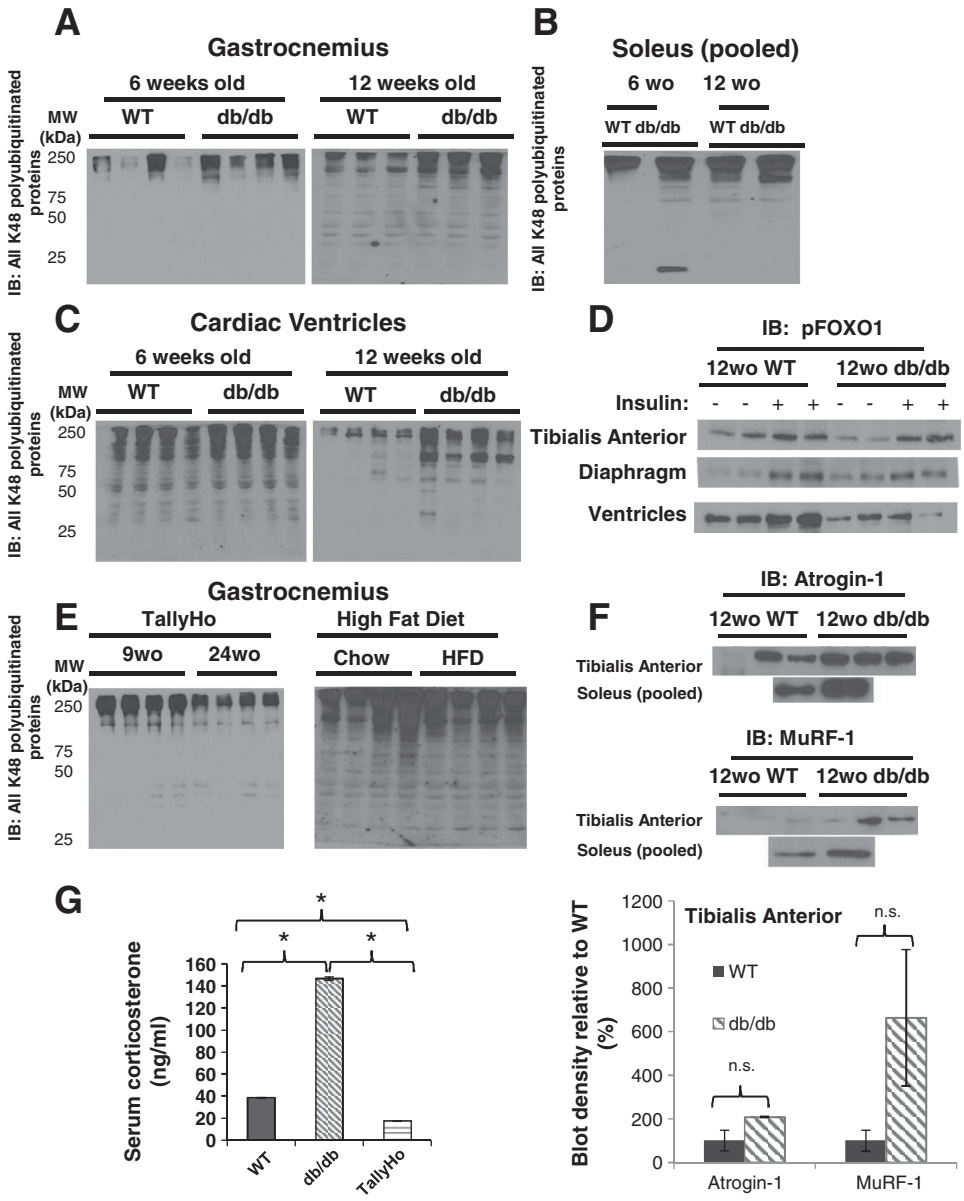

Fig. 5. Increased markers of protein degradation in insulin-resistant *db/db* muscle progresses in concert with the diabetes progression but is not evident in other models of type 2 diabetes mellitus (T2DM). Ubiquitin-conjugated protein levels are increased progressively compared with WT in prediabetic and diabetic *db/db* muscle that is predominantly fast/mixed twitch (gastrocnemius) (*A*), slow (soleus) (*B*), and cardiac (*C*). IB, immunoblot; MW, molecular mass. *D*: *db/db* muscle is resistant to insulin-dependent phosphorylation (associated with deactivation) of the transcription factor forkhead box O1 (FOXO1). Among the targets of FOXO1 transcriptional activation are MuRF-1 and atrogin-1 E3 ubiquitin ligases, which demonstrate a statistically insignificant trend toward increased protein expression in fast and slow 12-wk-old *db/db* skeletal muscle compared with age-matched WT controls (*F*). *E*: accumulation of ubiquitin-conjugated proteins is not increased with onset of the diabetic phenotype in TallyHo mice or high-fat diet (HFD)-induced obese mice. *G*: serum corticosterone levels are increased in *db/db* mice but decreased in TallyHo mice compared with WT C57BLKS/j controls. ns, Not significant. $^*P < 0.05$.

nated proteins were not significantly different in overtly diabetic TallyHo (24 wk old) compared with prediabetic TallyHo (24 wk old). In addition, no change in accumulation of polyubiquitinated proteins was evident in the HFD-fed obese mice compared with lean controls. These findings suggest that increased muscle accumulation of polyubiquitinated proteins is not a common feature to all models of insulin resistance or diabetes mellitus.

Increased Serum Corticosterone and Inflammatory Cytokines in db/db mice But Not TallyHo Mice

Morning serum corticosterone levels were elevated in *db/db* mice compared with WT C57BLKS/j age-matched controls. Serum corticosterone was reduced in TallyHo mice compared with both WT controls and *db/db* mice (Fig. 5*G*). This correlates well with the increased serum C5a, IL-4, and CXCL-9 seen in *db/db* mice but not in TallyHo mice (Table 2). Also, TNF-α was significantly reduced in TallyHo mice but not *db/db* mice compared with control mice. Finally, in cumulative analysis of all 39 inflammatory cytokine markers probed, *db/db* mice had a significantly higher mean level of inflammatory cytokines compared with both WT and TallyHo mice (WT = 100 ± 0%, *db/db* = 169 ± 28%, TallyHo = 104 ± 8%, $P < 0.05$).

Chronic Exercise Training Improves Exercise Capacity and Glucose Tolerance in db/db Mice

Voluntary physical activity of *db/db* mice, as quantified by interruption of in-cage horizontal infrared beams, was severely

Table 2. *Serum inflammatory cytokine profile of C57BLKS/j control, db/db, and TallyHo mice*

	Control (n = 3), %	*db/db* (n = 3), %	TallyHo (n = 5), %	WT vs. *db/db*	WT vs. TallyHo	*db/db* vs. TallyHo
BLC	100 ± 19	213 ± 156	66 ± 24	5.1×10^{-1}	3.7×10^{-1}	2.6×10^{-1}
C5/Ca	100 ± 7	97 ± 10	11 ± 6	8.5×10^{-1}	9.7×10^{-5}*	2.1×10^{-4}*
Eotaxin	100 ± 43	107 ± 52	110 ± 23	9.2×10^{-1}	8.3×10^{-1}	9.5×10^{-1}
G-CSF	100 ± 32	21 ± 3	55 ± 25	7.7×10^{-2}	3.8×10^{-1}	3.6×10^{-1}
GM-CSF	100 ± 44	103 ± 61	91 ± 16	9.7×10^{-1}	8.2×10^{-1}	8.2×10^{-1}
I-309	100 ± 26	96 ± 37	88 ± 21	9.4×10^{-1}	7.4×10^{-1}	8.4×10^{-1}
IFN-γ	100 ± 33	119 ± 83	165 ± 37	8.4×10^{-1}	2.8×10^{-1}	5.8×10^{-1}
IL-1α	100 ± 30	137 ± 53	116 ± 21	5.7×10^{-1}	6.6×10^{-1}	6.8×10^{-1}
IL-1β	100 ± 54	225 ± 198	125 ± 36	5.8×10^{-1}	7.0×10^{-1}	5.4×10^{-1}
IL-1 RA	100 ± 42	142 ± 67	83 ± 30	6.2×10^{-1}	7.5×10^{-1}	3.8×10^{-1}
IL-3	100 ± 40	280 ± 113	84 ± 26	2.1×10^{-1}	7.4×10^{-1}	7.1×10^{-2}
IL-4	100 ± 31	301 ± 90	34 ± 6	1.0×10^{-1}	3.4×10^{-2}*	6.8×10^{-3}*
IL-5	100 ± 39	111 ± 31	78 ± 15	8.4×10^{-1}	5.5×10^{-1}	3.2×10^{-1}
IL-6	100 ± 65	66 ± 31	57 ± 25	6.6×10^{-1}	4.9×10^{-1}	8.5×10^{-1}
IL-7	100 ± 56	198 ± 72	161 ± 33	3.5×10^{-1}	3.5×10^{-1}	6.2×10^{-1}
IL-10	100 ± 61	106 ± 80	71 ± 21	9.5×10^{-1}	6.0×10^{-1}	6.1×10^{-1}
IL-13	100 ± 34	131 ± 63	287 ± 95	6.9×10^{-1}	2.0×10^{-1}	2.9×10^{-1}
IL-16	100 ± 30	107 ± 42	80 ± 21	9.0×10^{-1}	6.0×10^{-1}	5.4×10^{-1}
IL-17	100 ± 46	149 ± 124	146 ± 41	7.3×10^{-1}	5.0×10^{-1}	9.8×10^{-1}
IL-23	100 ± 36	138 ± 70	58 ± 18	6.6×10^{-1}	2.8×10^{-1}	2.1×10^{-1}
IL-27	100 ± 44	146 ± 117	158 ± 50	7.3×10^{-1}	4.7×10^{-1}	9.2×10^{-1}
IP-10	100 ± 37	354 ± 154	128 ± 50	1.8×10^{-1}	7.1×10^{-1}	1.3×10^{-1}
I-TAC	100 ± 3	1,111 ± 873	135 ± 48	3.1×10^{-1}	6.0×10^{-1}	1.8×10^{-1}
JE CCL2/MCP-1	100 ± 17	150 ± 33	81 ± 22	2.5×10^{-1}	5.8×10^{-1}	1.2×10^{-1}
KC CXCL1	100 ± 28	148 ± 35	123 ± 41	3.4×10^{-1}	7.2×10^{-1}	6.9×10^{-1}
MCP-5	100 ± 46	125 ± 48	100 ± 27	7.3×10^{-1}	1.0×10^{0}	6.4×10^{-1}
M-CSF	100 ± 36	80 ± 32	105 ± 24	6.9×10^{-1}	9.0×10^{-1}	5.4×10^{-1}
MIG CXCL9	100 ± 19	160 ± 65	187 ± 21	4.2×10^{-1}	3.1×10^{-2}*	6.5×10^{-1}
MIP-1α	100 ± 36	165 ± 114	118 ± 27	6.1×10^{-1}	7.0×10^{-1}	6.2×10^{-1}
MIP-1β	100 ± 54	139 ± 94	97 ± 20	7.4×10^{-1}	9.6×10^{-1}	5.9×10^{-1}
MIP-2	100 ± 57	130 ± 70	99 ± 28	7.5×10^{-1}	9.9×10^{-1}	6.4×10^{-1}
RANTES	100 ± 42	123 ± 91	76 ± 19	8.3×10^{-1}	5.7×10^{-1}	5.4×10^{-1}
SDF-1	100 ± 31	65 ± 33	88 ± 21	4.8×10^{-1}	7.5×10^{-1}	5.5×10^{-1}
sICAM-1	100 ± 24	168 ± 72	163 ± 39	4.2×10^{-1}	3.0×10^{-1}	9.5×10^{-1}
TARC	100 ± 41	275 ± 183	84 ± 29	4.0×10^{-1}	7.6×10^{-1}	2.2×10^{-1}
TIMP-1	100 ± 22	100 ± 35	67 ± 20	9.9×10^{-1}	4.1×10^{-1}	4.1×10^{-1}
TNF-α	100 ± 45	27 ± 9	115 ± 21	1.8×10^{-1}	7.5×10^{-1}	2.4×10^{-2}*
TREM-1	100 ± 38	110 ± 49	72 ± 21	8.8×10^{-1}	5.0×10^{-1}	4.3×10^{-1}
Positive control	100 ± 14	91 ± 14	103 ± 6	6.6×10^{-1}	8.3×10^{-1}	3.8×10^{-1}
Average changes in inflammatory cytokine panel	100 ± 0	169 ± 28	104 ± 8	1.6×10^{-2}*	5.9×10^{-1}	2.8×10^{-2}*

The values are means normalized to WT protein expression levels ± SE; n, no. of mice. BLC, B lymphocyte chemoattractant; C-CSF, granulocyte macrophage colony-stimulating factor; IFN-γ, interferon-γ; IL-1 RA, interleukin-1 receptor antagonist; IP-10, interferon-γ-induced protein 10; I-TAC, interferon-inducible T cell α chemoattractant; MCP-1, monocyte chemotactic protein-1; KC, chemokine (C-X-C motif) ligand 1; M-CSF, macrophage colony-stimulating factor; MIG, monokine induced by interferon-γ; MIP, macrophage inflammatory protein; RANTES, rapid upon activation, normal T cell expressed and secreted; SDF, stromal cell-derived factor; sICAM-1, soluble intercellular adhesion molecule-1; TARC, thymus and activation-regulated chemokine; TIMP-1, tissue inhibitor of metalloproteinase-1; TNF-α, tumor necrosis factor-α; TREM-1, triggering receptor expressed on myeloid cells 1. Cumulative analysis of proteins studied shows that *db/db* mice had significantly higher levels of inflammatory cytokines compared with both WT and TalllyHo mice. In individual comparisons, significant increases in serum C5a, IL-4, and CXCL-9 were seen in *db/db* mice compared with WT. TNF-α was significantly reduced in TallyHo mice compared with WT. *$P < 0.05$ for indicated comparison.

reduced in 12-wk-old *db*/*db* mice compared with WT controls ($4.00 \times 10^5 \pm 1 \times 10^3$ beam breaks/day WT vs. $1.84 \times 10^5 \pm 4 \times 10^3$ beam breaks/day *db*/*db*, $P < 0.05$) (Fig. 6*A*). We hypothesized that decreased muscle activity may be sufficient to cause the observed reduction of muscle weight. To test if increased physical activity could reverse the muscle phenotype, we used chronic exercise, which is a treatment commonly prescribed for individuals with reduced muscle size and type 2 diabetes (2). Chronic forced treadmill training for 8 wk did not alter weight gain (Fig. 6*C*) but improved glucose tolerance (Fig. 6*D*) and increased maximum running speed (Fig. 6*E*) and maximum cardiac capacity ($\dot{V}O_{2max}$) (Fig. 6*F*). The exercise treatment did not increase the apparent size of hindlimb musculature and did not cause an increase in centrally located nuclei (Fig. 6*B*). Chronic exercise slightly increased the weight of the gastrocnemius muscle compared with sedentary *db*/*db* mice but did not rescue the muscle weight to healthy WT levels. However, the weight of the tibialis anterior muscle was not significantly increased by exercise (Table 1).

Chronic Exercise Reduces Levels of Ubiquitinated Proteins and Increases Akt Phosphorylation

On the biochemical level, chronic forced treadmill exercise for 8 wk was sufficient to reduce accumulation of polyubiquitinated proteins in *db*/*db* diabetic mice to levels similar to those seen in WT sedentary controls (Fig. 6*G*). Exercise-induced rescue of ubiquitination was accompanied by a significant reduction in atrogin-1 and a trend toward reduced MuRF-1 protein levels (Fig. 6*H*). Although total Akt protein levels are decreased in *db*/*db* mice, exercise did not rescue the Akt protein levels but did increase the level of Akt phosphorylation (Fig. 6*I*).

DISCUSSION

Early Onset of Reduced Muscle Size in db/db Mice

A key finding in *db*/*db* mice was that reduced skeletal muscle size and decreased running ability is already present at 5 wk of age, before the onset of chronic hyperglycemia (Fig. 1). This indicates that overt diabetes, chronic hyperglycemia, and comorbidities that accompany chronic diabetes [such as diabetic peripheral neuropathy (48) and diabetic nephropathy (10)] are not necessary for decreased muscle weight and function in this model. If the *db*/*db* muscle phenotype is representative of human diabetic muscle loss, this early decreased muscle size would suggest that insulin resistance may be sufficient to cause muscle atrophy before the onset of overt T2DM. Limited studies in young men ($n = 51$, ages 18–35) do indicate a positive correlation between insulin sensitivity and lean body mass study (61). However, further work must be done to establish if early insulin resistance is sufficient to cause muscle loss in prediabetic humans.

Alternatively, early decreased muscle size and function in *db*/*db* mice may not represent diabetic muscle loss but instead a failure of normal physiological skeletal muscle growth. Indeed, the early onset of decreased muscle size in *db*/*db* mice suggests that dysfunctional metabolism (e.g., altered leptin signaling, insulin resistance, and hyperlipidemia) during muscle development may create a growth-adverse environment in which normal muscle growth is stunted. In addition to glucose metabolism, insulin signaling interacts with critical growth-promoting and growth-permitting pathways [e.g., insulin-like growth factor-I (54), leptin (45), AMP-activated protein kinase, Akt, and mTOR] to integrate metabolic control and growth control (57). Indeed, conditional overexpression of constituitively active Akt1 has been shown to improve metabolic parameters in diet-induced insulin-resistant mice (21) and age-related insulin-resistant mice (1). Therefore, it is reasonable that the juvenile onset of insulin resistance, absent leptin signaling, and altered metabolism could compromise early muscle growth in the *db*/*db* mouse.

Additional evidence comes from the *ob*/*ob* mouse, which, like the *db*/*db* mouse, is leptin-signaling deficient and insulin resistant. The *ob*/*ob* mouse has normal gastrocnemius weight up to 2 wk of age, after which *ob*/*ob* muscle growth is stunted, with *ob*/*ob* muscle growing much more slowly than the WT muscle (41). Therefore, the reduced muscle mass seen in *ob*/*ob* and *db*/*db* mice is likely the result of a failure of physiological hypertrophy, rather than atrophy of a fully developed muscle. Although this diminished muscle growth could be because of the altered metabolic milieu caused by early insulin resistance [*db*/*db* have increased serum insulin levels by ~10 days of age (11)], it could also be caused by the combined effects of leptin (17, 45), lipotoxicity (59, 60), or deficient growth hormone signaling on skeletal muscle growth and metabolism.

From these data, it is reasonable to conclude that the juvenile onset of insulin resistance, decreased muscle size, and severe diabetes in the *db*/*db* mouse model may not accurately reflect the typical pattern of adult-onset diabetes and muscle atrophy of mature muscle seen in human patients with T2DM. These studies caution that future studies in leptin signaling-deficient models should take into account the presence of poor prediabetic muscle growth and verify findings in additional models of T2DM.

Muscle Growth and Function in Tallyho Mice Is Not Decreased

To expand our findings to a leptin-intact adult-onset model of T2DM, we also studied the TallyHo mouse model. The TallyHo mouse is a polygenic mature-onset model of severely hyperglycemic type 2 diabetes with intact leptin signaling, insulin resistance, and deficient muscle-specific glucose uptake (26). We were surprised to find no indication of muscle loss in the TallyHo mice; muscle weight increased with age (Table 1), and exercise capacity was maintained (Fig. 2) when comparing 2-mo-old (prediabetic) and 6-mo-old (overtly diabetic) mice (26). However, we cannot exclude that muscle mass and function could be affected in older TallyHo mice. The lack of observed muscle loss in TallyHo mice within the first 6 mo of life suggests that insulin resistance and chronic hyperglycemia alone are insufficient to cause rapid muscle loss in mice.

The heterogeneity of muscle phenotypes in models of T2DM is further shown in additional models of T2DM; high-fat diet-fed mice have mild increases in muscle size and no significant changes in skeletal muscle apoptosis, proteolysis, or autophagy compared with lean controls (60). The relatively mild diabetic phenotype of diet-induced obesity mice compared with humans and other models of T2DM may account for the paucity of muscle pathology in HFD-fed mice (38).

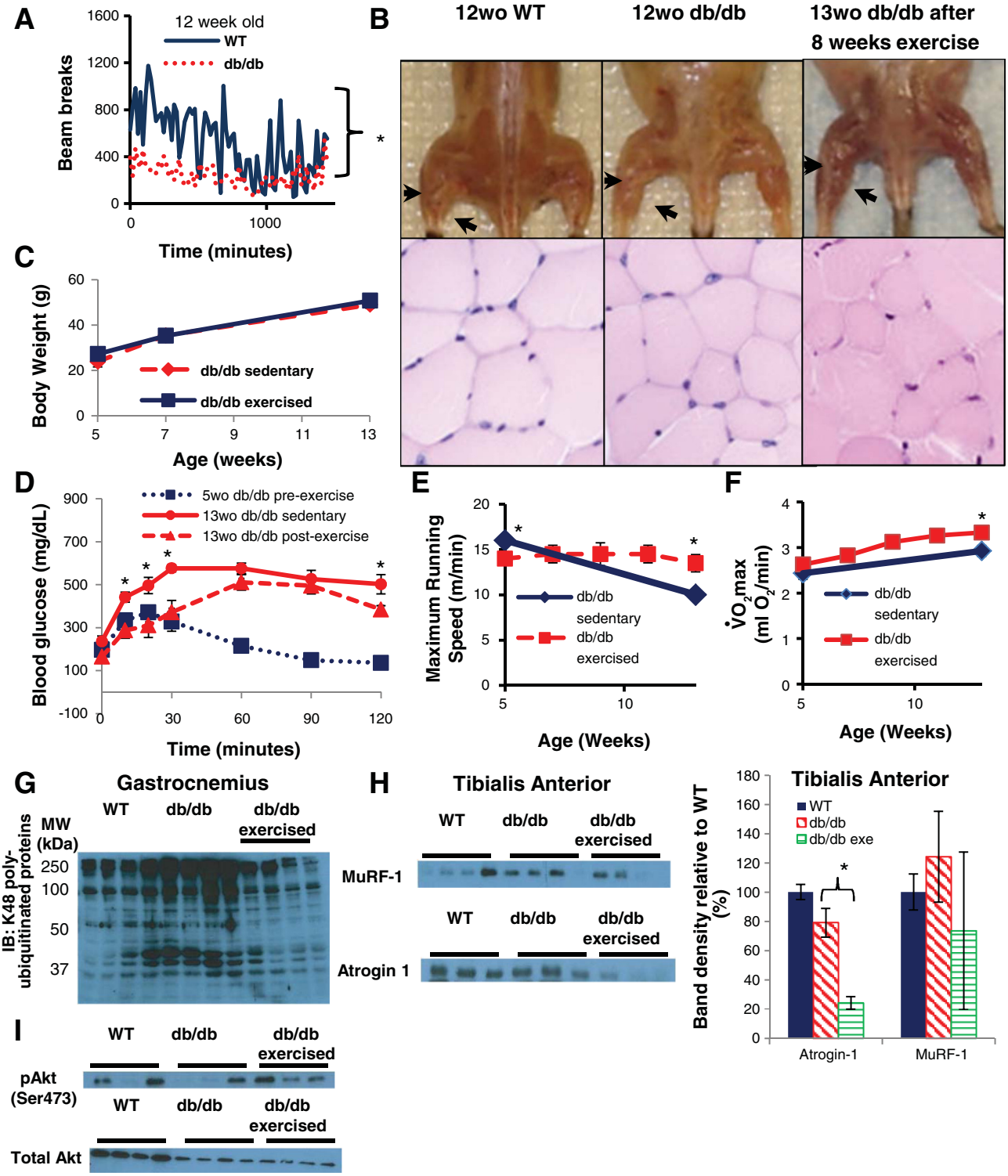

Fig. 6. Chronic interval training treadmill exercise of *db/db* mice for 8 wk moderately improves glucose tolerance and muscle phenotype. *A*: basal physical activity levels are decreased in 10-wk-old *db/db* mice compared with lean WT controls. *B*: gross and histological appearance of reduced muscle size are not visibly improved by exercise. *C*: weight gain is not altered by chronic exercise of *db/db* mice. *D*: exercise moderately increases glucose tolerance in exercised *db/db* mice compared with sedentary *db/db* controls. *E* and *F*: maximum running speed (*E*) and $\dot{V}O_{2max}$ (*F*) of exercised *db/db* mice are increased postexercise compared with nonexercised sedentary *db/db* controls. Chronic exercise was sufficient to reduce (G) K48 polyubiquitinated protein levels (*G*) and atrogin-1 ($P < 0.05$) and MuRF-1 ($P > 0.05$) levels (*H*). *I*: total Akt levels are decreased in *db/db* mice compared with WT mice, and, although exercise does not rescue total Akt levels, activating phosphorylation of Akt (pSer^{473}) is increased by exercise. Error bars, SE. *$P \leq 0.05$ compared with WT.

Additional mouse models with mutations of IRS-1/IRS-2, key signaling nodes in insulin signaling, have shown that, while independent loss of IRS-1 or IRS-2 has minimal effect on muscle growth and metabolism, dual mutations of IRS-1 and IRS-2 cause severely reduced muscle growth, insulin resistance, and impaired glycolytic metabolism (29). Thus, the observed differences between animal models of T2DM suggest that additional factors such as age of onset of diabetes, poor leptin signaling, degree of hyperinsulinemia, genetic strain, altered cytokine signaling, and differing diabetes-associated comorbidities may dictate the effects of diabetes on muscle growth and maintenance. These findings together with studies showing improved muscle phenotypes with treatment of diabetes in *db*/*db* mice (62) and humans (14, 36, 37) suggest that T2DM acts to exacerbate muscle loss instigated by other factors (e.g., age, injury, disuse, and chronic disease).

Increased Glucocorticoid and Inflammatory Signaling Correlates with Decreased Muscle Size and Function in Insulin-Resistant Mice

Previous studies have shown that intact glucocorticoid signaling is necessary for the rapid muscle loss that occurs in streptozotocin-induced T1DM (19). Our results suggest that glucocorticoid and inflammatory signaling are similarly important in muscle loss in T2DM. Indeed, in the T2DM mouse model with poor muscle size and function (*db*/*db*), corticosterone and inflammatory cytokine signaling are increased (Fig. 5*G* and Table 2). Conversely, in the T2DM mouse model with intact muscle growth and function (TallyHo), serum corticosterone was actually lower than control mice. These findings suggest a positive correlation between increased glucocorticoid/inflammatory signaling and poor muscle growth/function in T2DM that could be targeted therapeutically. However, further work employing genetic and pharmacological approaches must be done to determine if increased glucocorticoid signaling is essential to muscle loss in individuals with T2DM.

Insulin-Dependent Protein Synthesis Is Severely Blunted in db/db Mice

To understand the basis for decreased muscle size in *db*/*db* mice, we studied biochemical markers of protein synthesis and the level of polyubiquitinated proteins destined for proteasomal degradation. Several human studies indicate that, in diabetes, whereas meal-induced protein synthesis is normal, protein degradation is increased and drives net protein loss, although the findings are inconsistent [type 1 diabetes (12, 35, 40, 51) and type 2 diabetes (5, 62)]. Our findings of blunted insulin-dependent phosphorylation of regulators of protein synthesis (Akt, mTOR, p70S6K, S6, and 4EBP-1) in slow, mixed, fast, and cardiac muscle types of 12-wk-old *db*/*db* mice suggest that insulin resistance may decrease insulin-dependent protein synthesis and contribute to decreased muscle size (Fig. 4). These findings may differ from human studies (30) measuring meal-induced protein synthesis because the use of carbohydrate or protein ingestion to induce protein synthesis allows for compensatory hyperinsulinemia, which may be sufficient to normalize protein synthesis in insulin-resistant individuals. In contrast, the direct intraperitoneal administration of insulin studied here in *db*/*db* mice compares responses to equivalent increases in insulin.

Markers of Protein Degradation in Insulin-Resistant Mice

Previous studies in *db*/*db* mice showed that the rate of muscle protein degradation is increased, as measured by ex vivo tyrosine release (62). This finding is further supported by our observations in *db*/*db* mice of decreased insulin-dependent FOXO1 phosphorylation, increased atrophy-associated E3 ubiquitin ligase expression (i.e., MuRF-1 and atrogin-1), and increased accumulation of K48-polyubiquitin-conjugated proteins (Fig. 5). Wang et al.(62) observed increased proteasomal chymotrypic-like peptidase function in muscle from 9-wk-old *db*/*db* mice, suggesting that the increase we observed in ubiquitin-conjugated protein is caused by an increased rate of ubiquitination, rather than by decreased proteasomal function. Moreover, accumulation of ubiquitin-conjugated proteins has been closely linked with increased muscle protein degradation rates during starvation and denervation muscle atrophy (64). This increase of ubiquitinated proteins was already evident in slow, fast, and cardiac muscle from young prediabetic *db*/*db* mice and further increased in overtly diabetic *db*/*db* mice, suggesting that increased muscle protein degradation is a global *db*/*db* muscle phenomenon and contributes to the poor muscle growth present in skeletal muscle from *db*/*db* mice. On the other hand, accumulation of ubiquitinated proteins was not evident in gastrocnemius muscle of HFD-fed mice or Tallyho mice, suggesting that factors other than insulin resistance and chronic hyperglycemia may be responsible for increased levels of ubiquitinated proteins.

Exercise Training of db/db Mice Improves Muscle Function and Glucose Tolerance

When muscle loss in patients interferes with physical function, chronic exercise is a treatment commonly prescribed to increase muscle function, muscle mass, and to improve glucose tolerance. Although chronic exercise of *db*/*db* mice improved glucose tolerance, cardiac capacity ($\dot{V}O_{2max}$), and running speeds, only a mild increase in final muscle weight was observed in exercised compared with nonexercised *db*/*db* mice, indicating that exercise is insufficient to fully rescue muscle growth in the *db*/*db* mouse model. This suggests that decreased muscle use (Fig. 6*A*) is not the basis for the reduced muscle size of *db*/*db* mice. Despite the inability to completely rescue muscle growth, exercise was sufficient to increase basal Akt Ser^{473} phosphorylation and reduce both MuRF-1 expression and accumulation of polyubiquitinated proteins (Fig. 6, *G–I*). This suggests that decreased protein degradation and increased protein synthesis was responsible for the mild increase in muscle weight in the exercised *db*/*db* mice. Moreover, these findings support the current clinical use of exercise to improve glucose tolerance, muscle function, and exercise capacity.

In summary, our studies in the *db*/*db* and TallyHo mouse models suggest that the effects of type 2 diabetes on muscle mass and function are model-dependent and correlate with glucocorticoid and inflammatory signaling. The reduced muscle size in *db*/*db* mice before the onset of overt hyperglycemia and diabetes suggests that the *db*/*db* mouse model is an extreme model of diabetes in which the altered metabolic milieu caused by insulin resistance and defective leptin signaling may be toxic to early muscle growth. The lack of decreased muscle mass and exercise capacity in the TallyHo mice sug-

gests that insulin resistance and chronic hyperglycemia alone are insufficient alone to cause rapidly decreased muscle size and function. It is likely that additional factors such as genetic background, hyperinsulinemia, lipotoxicity, leptin signaling, age of onset, and diabetic comorbidities influence whether the metabolic milieu is toxic to or supportive of growth and maintenance of skeletal muscle in T2DM.

ACKNOWLEDGMENTS

We thank Leslie Rowland, Meghna Pant, and Drs. Martha Belury, Denis Guttridge, Jonathan Davis, and Peter Reiser for contributing ideas and providing critical feedback for this work.

GRANTS

This research was supported financially by the American Diabetes Association (7-11-CST-02) and the Heart, Lung, and Blood Institute of the National Institutes of Health under award number NIH-RO1-HL-088555.

DISCLOSURES

No conflicts of interest, financial or otherwise, are declared by the authors.

AUTHOR CONTRIBUTIONS

J.E.O., S.K.M., J.D., S.R.R., S.T.D., M.T.Z., and M.P. conception and design of research; J.E.O., S.K.M., J.D., and S.R.R. performed experiments; J.E.O., S.K.M., J.D., S.R.R., S.T.D., and M.P. analyzed data; J.E.O., S.K.M., J.D., S.R.R., M.T.Z., and M.P. interpreted results of experiments; J.E.O., S.K.M., and J.D. prepared figures; J.E.O. drafted manuscript; J.E.O., S.K.M., J.D., S.R.R., S.T.D., M.T.Z., and M.P. edited and revised manuscript; J.E.O., S.K.M., J.D., S.R.R., S.T.D., M.T.Z., and M.P. approved final version of manuscript.

REFERENCES

1. **Akasaki Y, Ouchi N, Izumiya Y, Bernardo BL, Lebrasseur NK, Walsh K.** Glycolytic fast-twitch muscle fiber restoration counters adverse age-related changes in body composition and metabolism. *Aging Cell* 13: 80–91, 2014.
2. **Albright A, Franz M, Hornsby G, Kriska A, Marrero D, Ulrich L, Verity L.** American College of Sports Medicine position stand. Exercise and type 2 diabetes. *Med Sci Sports Exerc* 32: 1345–1360, 2000.
3. **Almond RE, Enser M.** A histochemical and morphological study of skeletal muscle from obese hyperglycaemic *ob/ob* mice. *Diabetologia* 27: 407–413, 1984.
4. **Bal NC, Maurya SK, Sopariwala DH, Sahoo SK, Gupta SC, Shaikh SA, Pant M, Rowland LA, Bombardier E, Goonasekera SA, Tupling AR, Molkentin JD, Periasamy M.** Sarcolipin is a newly identified regulator of muscle-based thermogenesis in mammals. *Nat Med* 18: 1575–1579, 2012.
5. **Bell JA, Volpi E, Fujita S, Cadenas JG, Sheffield-Moore M, Rasmussen BB.** Skeletal muscle protein anabolic response to increased energy and insulin is preserved in poorly controlled type 2 diabetes. *J Nutr* 136: 1249–1255, 2006.
6. **Bodine SC, Latres E, Baumhueter S, Lai VKM, Nunez L, Clarke BA, Poueymirou WT, Panaro FJ, Na E, Dharmarajan K, Pan ZQ, Valenzuela DM, DeChiara TM, Stitt TN, Yancopoulos GD, Glass DJ.** Identification of ubiquitin ligases required for skeletal muscle atrophy. *Science* 294: 1704–1708, 2001.
7. **Bruton J, Katz A, Abbate F, Westerblad H.** Regulation of myoplasmic Ca 2+ in genetically obese (*ob/ob*) mouse single skeletal muscle fibres. *Pflugers Arch* 444: 692–699, 2002.
8. **Centers for Disease Control, and Prevention.** *National Diabetes Fact Sheet: National Estimates and General Information on Diabetes and Prediabetes in the United States, 2011*. Atlanta, GA: U.S. Department of Health and Human Services, Center for Disease Control and Prevention, 2011.
9. **Chick W, Lavine R, Like A.** Studies in the diabetic mutant mouse: V. Glucose tolerance in mice homozygous and heterozygous for the diabetes gene. *Diabetologia* 6: 257–262, 1970.
10. **Chow F, Ozols E, Nikolic-Paterson DJ, Atkins RC, Tesch GH.** Macrophages in mouse type 2 diabetic nephropathy: Correlation with diabetic state and progressive renal injury. *Kidney Int* 65: 116–128, 2004.
11. **Coleman DL, Hummel KP.** Hyperinsulinemia in pre-weaning diabetes (db) mice. *Diabetologia* 10: 607–610, 1974.
11a. **De Rekeneire N, Resnick HE, Schwartz AV, Shorr RI, Kuller LH, Simonsick EM, Vellas B, Harris TB.** Diabetes is associated with subclinical functional limitation in nondisabled older individuals: the Health, Aging, and Body Composition study. *Diabetes Care* 26: 3257–3263, 2003.
12. **Dice JF, Walker CD, Byrne B, Cardiel A.** General characteristics of protein degradation in diabetes and starvation. *Proc Natl Acad Sci USA* 75: 2093–2097, 1978.
13. **Gapp DA, Leiter EH, Coleman DL, Schwizer RW.** Temporal changes in pancreatic islet composition in C57BL/6J-*db/db* (diabetes) mice. *Diabetologia* 25: 439–443, 1983.
14. **Goodpaster BH, Park SW, Harris TB, Kritchevsky SB, Nevitt M, Schwartz AV, Simonsick EM, Tylavsky FA, Visser M, Newman AB.** The loss of skeletal muscle strength, mass, and quality in older adults: the health, aging and body composition study. *J Gerontol A Biol Sci Med Sci* 61: 1059–1064, 2006.
15. **Gregg EW, Beckles GL, Williamson DF, Leveille SG, Langlois JA, Engelgau MM, Narayan KM.** Diabetes and physical disability among older US adults. *Diabetes Care* 23: 1272–1277, 2000.
16. **Halvatsiotis P, Short KR, Bigelow M, Nair KS.** synthesis rate of muscle proteins, muscle functions, and amino acid kinetics in type 2 diabetes. *Diabetes* 51: 2395–2404, 2002.
17. **Hamrick MW, Herberg S, Arounleut P, He HZ, Shiver A, Qi RQ, Zhou L, Isales CM, Mi QS.** The adipokine leptin increases skeletal muscle mass and significantly alters skeletal muscle miRNA expression profile in aged mice. *Biochem Biophys Res Commun* 400: 379–383, 2010.
18. **Hu Z, Lee IH, Wang X, Sheng H, Zhang L, Du J, Mitch WE.** PTEN expression contributes to the regulation of muscle protein degradation in diabetes. *Diabetes* 56: 2449–2456, 2007.
19. **Hu Z, Wang H, Lee IH, Du J, Mitch WE.** Endogenous glucocorticoids and impaired insulin signaling are both required to stimulate muscle wasting under pathophysiological conditions in mice. *J Clin Invest* 119: 3059–3069, 2009.
20. **Ingalls AM, Dickie MM, Snell GD.** Obese, a new mutation in the house mouse. *J Hered* 41: 317–318, 1950.
21. **Izumiya Y, Hopkins T, Morris C, Sato K, Zeng L, Viereck J, Hamilton JA, Ouchi N, LeBrasseur NK, Walsh K.** Fast/glycolytic muscle fiber growth reduces fat mass and improves metabolic parameters in obese mice. *Cell Metab* 7: 159–172, 2008.
22. **Janssen I, Heymsfield SB, Ross R.** Low relative skeletal muscle mass (sarcopenia) in older persons is associated with functional impairment and physical disability. *J Am Geriatr Soc* 50: 889–896, 2002.
23. **Kawasaki F, Matsuda M, Kanda Y, Inoue H, Kaku K.** Structural and functional analysis of pancreatic islets preserved by pioglitazone in *db/db* mice. *Am J Physiol Endocrinol Metab* 288: E510–E518, 2005.
24. **Kemp JG, Blazev R, Stephenson DG, Stephenson GMM.** Morphological and biochemical alterations of skeletal muscles from the genetically obese (*ob/ob*) mouse. *Int J Obes* 33: 831–841, 2009.
25. **Kim JH, Saxton AM.** The TALLYHO mouse as a model of human type 2 diabetes. In: *Animal Models in Diabetes Research*, edited by Joost H-G, Al-Hasani H, Schürmann A. Clifton, NJ: Humana, p. 75–87, 2013.
26. **Kim JH, Stewart TP, Soltani-Bejnood M, Wang L, Fortuna JM, Mostafa OA, Moustaid-Moussa N, Shoieb AM, McEntee MF, Wang Y, Bechtel L, Naggert JK.** Phenotypic characterization of polygenic type 2 diabetes in TALLYHO/JngJ mice. *J Endocrinol* 191: 437–446, 2006.
27. **Kim TN, Park MS, Yang SJ, Yoo HJ, Kang HJ, Song W, Seo JA, Kim SG, Kim NH, Baik SH, Choi DS, Choi KM.** Prevalence and determinant factors of sarcopenia in patients with type 2 diabetes: the korean sarcopenic obesity study (KSOS). *Diabetes Care* 33: 1497–1499, 2010.
28. **Koproski J, Pretto Z, Poretsky L.** Effects of an intervention by a diabetes team in hospitalized patients with diabetes. *Diabetes Care* 20: 1553–1555, 1997.
29. **Long YC, Cheng Z, Copps KD, White MF.** Insulin receptor substrates Irs1 and Irs2 coordinate skeletal muscle growth and metabolism via the Akt and AMPK pathways. *Mol Cell Biol* 31: 430–441, 2011.
30. **Manders RJ, Koopman R, Beelen M, Gijsen AP, Wodzig WK, Saris WH, Loon van LJ.** The muscle protein synthetic response to carbohydrate and protein ingestion is not impaired in men with longstanding type 2 diabetes. *J Nutr* 138: 1079–1085, 2008.
31. **Maurer MS, Burcham J, Cheng H.** Diabetes mellitus is associated with an increased risk of falls in elderly residents of a long-term care facility. *J Gerontol A Biol Sci Med Sci* 60: 1157–1162, 2005.

32. **Morley JE.** Sarcopenia: diagnosis and treatment. *J Nutr Health Aging* 12: 452–456, 2008.
33. **Nguyen MH, Cheng M, Koh TJ.** Impaired muscle regeneration in *ob*/*ob* and *db*/*db* mice. *Sci World J* 11: 1525–1535, 2011.
34. **O'Neill ED, Wilding JPH, Kahn CR, Van Remmen H, McArdle A, Jackson MJ, Close GL.** Absence of insulin signalling in skeletal muscle is associated with reduced muscle mass and function: evidence for decreased protein synthesis and not increased degradation. *Age Dordr Neth* 32: 209–222, 2010.
35. **Pain VM, Albertse EC, Garlick PJ.** Protein metabolism in skeletal muscle, diaphragm, and heart of diabetic rats. *Am J Physiol Endocrinol Metab* 245: E604–E610, 1983.
36. **Park SW, Goodpaster BH, Lee JS, Kuller LH, Boudreau R, de Rekeneire N, Harris TB, Kritchevsky S, Tylavsky FA, Nevitt M, others.** Excessive loss of skeletal muscle mass in older adults with type 2 diabetes. *Diabetes Care* 32: 1993–1997, 2009.
37. **Park SW, Goodpaster BH, Strotmeyer ES, Kuller LH, Broudeau R, Kammerer C, de Rekeneire N, Harris TB, Schwartz AV, Tylavsky FA, others.** Accelerated loss of skeletal muscle strength in older adults with type 2 diabetes the health, aging, and body composition study. *Diabetes Care* 30: 1507–1512, 2007.
38. **Park SY, Cho YR, Kim HJ, Higashimori T, Danton C, Lee MK, Dey A, Rothermel B, Kim YB, Kalinowski A, Russell KS, Kim JK.** Unraveling the temporal pattern of diet-induced insulin resistance in individual organs and cardiac dysfunction in c57bl/6 mice. *Diabetes* 54: 3530–3540, 2005.
39. **Pepato MT, Migliorini RH, Goldberg AL, Kettelhut IC.** Role of different proteolytic pathways in degradation of muscle protein from streptozotocin-diabetic rats. *Am J Physiol Endocrinol Metab* 271: E340–E347, 1996.
40. **Price SR, Bailey JL, Wang X, Jurkovitz C, England BK, Ding X, Phillips LS, Mitch WE.** Muscle wasting in insulinopenic rats results from activation of the ATP-dependent, ubiquitin-proteasome proteolytic pathway by a mechanism including gene transcription. *J Clin Invest* 98: 1703–1708, 1996.
41. **Purchas RW, Romsos DR, Allen RE, Merkel RA.** Muscle growth and satellite cell proliferative activity in obese (*ob*/*ob*) mice. *J Anim Sci* 60: 644–651, 1985.
42. **Rasband WS.** *ImageJ*. Bethesda, MD: Natl. Institutes of Health.
44. **Ryerson B, Tierney EF, Thompson TJ, Engelgau MM, Wang J, Gregg EW, Geiss LS.** Excess physical limitations among adults with diabetes in the U.S population, 1997–1999. *Diabetes Care* 26: 206–210, 2003.
45. **Sáinz N, Rodríguez A, Catalán V, Becerril S, Ramírez B, Gómez-Ambrosi J, Frühbeck G.** Leptin administration favors muscle mass accretion by decreasing Foxo3a and increasing PGC-1α in *ob*/*ob* mice. *PLoS ONE* 4: e6808, 2009.
46. **Schwartz MW, Baskin DG, Bukowski TR, Kuijper JL, Foster D, Lasser G, Prunkard DE, Porte D, Woods SC, Seeley RJ, Weigle DS.** Specificity of leptin action on elevated blood glucose levels and hypothalamic neuropeptide y gene expression in *ob*/*ob* mice. *Diabetes* 45: 531–535, 1996.
47. **Shao J, Yamashita H, Qiao L, Friedman JE.** Decreased Akt kinase activity and insulin resistance in C57BL/KsJ-Leprdb/db mice. *J Endocrinol* 167: 107–115, 2000.
48. **Sima AAF, Robertson DM.** Peripheral neuropathy in mutant diabetic mouse [C57BL/Ks (*db*/*db*)]. *Acta Neuropathol (Berl)* 41: 85–89, 1978.
49. **Singh MAF, Singh NA, Hansen RD, Finnegan TP, Allen BJ, Diamond TH, Diwan AD, Lloyd BD, Williamson DA, Smith EUR, Grady JN, Stavrinos TM, Thompson MW.** Methodology and baseline characteristics for the sarcopenia and hip fracture study: a 5-year prospective study. *J. Gerontol. A. Biol. Sci. Med. Sci*. 64A: 568–574, 2009.
50. **Sitnick M, Bodine SC, Rutledge JC.** Chronic high fat feeding attenuates load-induced hypertrophy in mice. *J Physiol* 587: 5753–5765, 2009.
51. **Smith OLK, Wong CY, Gelfand RA.** Skeletal muscle proteolysis in rats with acute streptozocin-induced diabetes. *Diabetes* 38: 1117–1122, 1989.
52. **Stewart TP, Kim HY, Saxton AM, Kim JH.** Genetic and genomic analysis of hyperlipidemia, obesity and diabetes using (C57BL/6J × TALLYHO/JngJ) F2 mice (Abstract). *BMC Genomics* 11: 713, 2010.
53. **Stickland NC, Batt RA, Crook AR, Sutton CM.** Inability of muscles in the obese mouse (*ob*/*ob*) to respond to changes in body weight and activity. *J Anat* 184: 527–533, 1994.
54. **Stitt TN, Drujan D, Clarke BA, Panaro F, Timofeyva Y, Kline WO, Gonzalez M, Yancopoulos GD, Glass DJ.** The IGF-1/PI3K/Akt pathway prevents expression of muscle atrophy-induced ubiquitin ligases by inhibiting foxo transcription factors. *Mol Cell* 14: 395–403, 2004.
55. **Støllen TO, Høydal MA, Kemi OJ, Catalucci D, Ceci M, Aasum E, Larsen T, Rolim N, Condorelli G, Smith GL, Wisløff U.** Interval training normalizes cardiomyocyte function, diastolic Ca2+ control, and Sr Ca2+ release synchronicity in a mouse model of diabetic cardiomyopathy. *Circ Res* 105: 527–536, 2009.
56. **Strotmeyer ESCJ.** Nontraumatic fracture risk with diabetes mellitus and impaired fasting glucose in older white and black adults: the health, aging, and body composition study. *Arch Intern Med* 165: 1612–1617, 2005.
57. **Taniguchi CM, Emanuelli B, Kahn CR.** Critical nodes in signalling pathways: insights into insulin action. *Nat Rev Mol Cell Biol* 7: 85–96, 2006.
58. **Tomita T, Doull V, Pollock HG, Krizsan D.** Pancreatic islets of obese hyperglycemic mice (*ob*/*ob*). *Pancreas* 7: 367–375, 1992.
59. **Turpin SM, Lancaster GI, Darby I, Febbraio MA, Watt MJ.** Apoptosis in skeletal muscle myotubes is induced by ceramides and is positively related to insulin resistance. *Am J Physiol Endocrinol Metab* 291: E1341–E1350, 2006.
60. **Turpin SM, Ryall JG, Southgate R, Darby I, Hevener AL, Febbraio MA, Kemp BE, Lynch GS, Watt MJ.** Examination of "lipotoxicity" in skeletal muscle of high-fat fed and *ob*/*ob* mice. *J Physiol* 587: 1593–1605, 2009.
61. **Unni US, Ramakrishnan G, Raj T, Kishore RP, Thomas T, Vaz M, Kurpad AV.** Muscle mass and functional correlates of insulin sensitivity in lean young Indian men. *Eur J Clin Nutr* 63: 1206–1212, 2009.
62. **Wang X, Hu Z, Hu J, Du J, Mitch WE.** Insulin resistance accelerates muscle protein degradation: activation of the ubiquitin-proteasome pathway by defects in muscle cell signaling. *Endocrinology* 147: 4160–4168, 2006.
63. **Warmington SA, Tolan R, McBennett S.** Functional and histological characteristics of skeletal muscle and the effects of leptin in the genetically obese (*ob*/*ob*) mouse. *Int J Obes Relat Metab Disord J Int Assoc Study Obes* 24: 1040–1050, 2000.
64. **Wing SS, Haas AL, Goldberg AL.** Increase in ubiquitin-protein conjugates concomitant with the increase in proteolysis in rat skeletal muscle during starvation and atrophy denervation. *Biochem J* 307: 639–645, 1995.
65. **Yokota T, Kinugawa S, Hirabayashi K, Matsushima S, Inoue N, Ohta Y, Hamaguchi S, Sobirin MA, Ono T, Suga T, Kuroda S, Tanaka S, Terasaki F, Okita K, Tsutsui H.** Oxidative stress in skeletal muscle impairs mitochondrial respiration and limits exercise capacity in type 2 diabetic mice. *Am J Physiol Heart Circ Physiol* 297: H1069–H1077, 2009.